 Inorg. Chem. **2009,** *48,* 4952–4962
DOI:10.1021/ic900389z

Inorganic Chemistry
Article

Visible Light-Driven Hydrogen Production from Aqueous Protons Catalyzed by Molecular Cobaloxime Catalysts

Pingwu Du, Jacob Schneider, Genggeng Luo, William W. Brennessel, and Richard Eisenberg*

Department of Chemistry, University of Rochester, Rochester, New York 14627

Received February 25, 2009

A series of cobaloxime complexes—([Co(dmgH)$_2$pyCl] (**1**), [Co(dmgH)$_2$(4-COOMe-py)Cl] (**2**), [Co(dmgH)$_2$(4-Me$_2$N-py)Cl] (**3**), [Co(dmgH)(dmgH$_2$)Cl$_2$] (**4**), [Co(dmgH)$_2$(py)$_2$](PF$_6$) (**5**), [Co(dmgH)$_2$(P(*n*-Bu)$_3$)Cl] (**6**), and [Co(dmgBF$_2$)$_2$(OH$_2$)$_2$] (**7**), where dmgH = dimethylglyoximate monoanion, dmgH$_2$ = dimethylglyoxime, dmgBF$_2$ = (difluoroboryl)dimethylglyoximate anion, and py = pyridine—were synthesized and studied as molecular catalysts for the photogeneration of hydrogen from systems containing a Pt terpyridyl acetylide chromophore and triethanolamine (TEOA) as a sacrificial donor in aqueous acetonitrile. All cobaloxime complexes **1**−**7** are able to quench the luminescence of the Pt(II) chromophore [Pt(ttpy)(C≡CPh)]ClO$_4$ (**C1**) (ttpy = 4′-*p*-tolyterpyridine). The most effective electron acceptor for hydrogen evolution is found to be complex **2**, which provides the fastest luminescence quenching rate constant for **C1** of 1.7×10^9 M^{-1} s^{-1}. The rate of hydrogen evolution depends on many factors, including the stability of the catalysts, the driving force for proton reduction, the relative and absolute concentrations of system components (TEOA, Co molecular catalyst, and sensitizer), and the ratio of MeCN/water in the reaction medium. For example, when the concentration of TEOA increases, the rate of H_2 photogeneration is faster and the induction period is shorter. Colloidal cobalt experiments and mercury tests were run to verify that the system is homogeneous and that catalysis does not occur from in situ generated colloidal particles during photolysis. The most effective system examined to date consists of the chromophore **C1** (1.1×10^{-5} M), TEOA (0.27 M), and catalyst complex **1** (2.0×10^{-4} M) in a MeCN/water mixture (24:1 v/v, total 25 mL); this system has produced ∼2150 turnovers of H_2 after only 10 h of photolysis with $\lambda > 410$ nm.

Introduction

The development of renewable energy from the sun is a major challenge in addressing the problem of abundant and environmentally benign energy for sustainable development globally.[1−8] A promising energy conversion pathway considered by many researchers is the development of efficient catalytic systems that can convert the energy of solar photons into stored chemical potential by splitting water into hydrogen and oxygen. Hydrogen with its high specific enthalpy of combustion, its use in fuel cells, and its benign combustion product (water) is the ideal fuel to be produced using solar energy, and it will serve to reduce mankind's dependence on fossil fuels and subsequent emissions of the greenhouse gases.

Colloidal platinum is a well-known heterogeneous catalyst for hydrogen production. Numerous successful systems to produce H_2 have been constructed utilizing colloidal platinum nanoparticles in combination with different chromophores, such as Ru(bpy)$_3^{2+}$,[3,9−11] Zn(II) porphyrins,[12−15] platinum(II) terpyridyl acetylide complexes,[16,17] cyclometalated [Ir(C^N)2(N^N)]PF$_6$ complexes,[18−20]

*To whom correspondence should be addressed. E-mail: eisenberg@chem.rochester.edu.

(1) Bard, A. J.; Fox, M. A. *Acc. Chem. Res.* **1995**, *28*, 141–145.
(2) Chakraborty, S.; Wadas, T. J.; Hester, H.; Schmehl, R.; Eisenberg, R. *Inorg. Chem.* **2005**, *44*, 6865–6878.
(3) Grätzel, M. *Acc. Chem. Res.* **1981**, *14*, 376–384.
(4) Grätzel, M. *Inorg. Chem.* **2005**, *44*, 6841–6851.
(5) Alstrum-Acevedo, J. H.; Brennaman, M. K.; Meyer, T. J. *Inorg. Chem.* **2005**, *44*, 6802–6827.
(6) Esswein, A. J.; Nocera, D. G. *Chem. Rev.* **2007**, *107*, 4022–4047.
(7) Lewis, N. S.; Nocera, A. G. *Proc. Natl. Acad. Sci. U.S.A.* **2006**, *103*, 15729–15735.
(8) Eisenberg, R.; Nocera, D. G. *Inorg. Chem.* **2005**, *44*, 6799–6801.
(9) Kalyanasundaram, K.; Kiwi, J.; Gratzel, M. *Helv. Chim. Acta* **1978**, *61*, 2720–2730.
(10) Kirch, M.; Lehn, J.-M.; Sauvage, J.-P. *Helv. Chim. Acta* **1979**, *62*, 1345–1384.
(11) Lehn, J.-M.; Sauvage, J.-P. *Nouv. J. Chim.* **1977**, *1*, 449–451.
(12) Adar, E.; Degani, Y.; Goren, Z.; Willner, I. *J. Am. Chem. Soc.* **1986**, *108*, 4696–4700.
(13) Okura, I. *Coord. Chem. Rev.* **1985**, *68*, 53.
(14) Okura, I.; Kaji, N.; Aono, S.; Kita, T. *Inorg. Chem.* **1985**, *24*, 451–453.
(15) Okura, I.; Kim-Thuan, N. *J. Mol. Catal.* **1979**, *6*, 227–230.
(16) Du, P.; Schneider, J.; Jarosz, P.; Eisenberg, R. *J. Am. Chem. Soc.* **2006**, *128*, 7726–7727.
(17) Du, P.; Schneider, J.; Jarosz, P.; Zhang, J.; Brennessel, W. W.; Eisenberg, R. *J. Phys. Chem. B* **2007**, *111*, 6887–6894.
(18) Goldsmith, J. I.; Hudson, W. R.; Lowry, M. S.; Anderson, T. H.; Bernhard, S. *J. Am. Chem. Soc.* **2005**, *127*, 7502–7510.
(19) Grzybowski, J. J.; Urbach, F. L. *Inorg. Chem.* **1980**, *19*, 2604–2608.
(20) Lowry, M. S.; Goldsmith, J. I.; Slinker, J. D.; Rohl, R.; Pascal, J. R. A.; Malliaras, G. G.; Bernhard, S. *Chem. Mater.* **2005**, *17*, 5712–5719.

 Published on Web 4/27/2009

halogenated fluorescein dyes,[21−23] methyl acridine orange,[24] and conjugated polymers.[25] However, due to the high price of platinum metal, many researchers are exploring earth-abundant, less expensive catalysts such as cobalt, nickel, and iron complexes[26−31] to replace the colloidal platinum catalyst. Early studies reported the successful use of $Co(bpy)_3^{2+}$ as a hydrogen-generating catalyst to replace colloidal platinum in systems using $Ru(bpy)_3^{2+}$ and, more recently, $[Ir(ppy)_2(bpy)]^{2+}$ photosensitizers.[18,32] Within the past decade, cobaloximes (cobaloximes are bis(dialkyl or diarylglyoximate)cobalt complexes) have been reported for hydrogen production based initially on electrocatalytic studies[28−31] and extended more recently to photochemical investigations.[33−36] In the earlier studies, Artero and Peters and their respective co-workers reported that $Co(dmgBF_2)_2$ ($dmgBF_2$ = difluoroboryldimethylglyoximate) can electrocatalytically produce hydrogen at an impressively low overpotential of 50 mV in acetonitrile in the presence of CF_3COOH and also generate hydrogen using other acids (such as tosic acid, p-cyanoanilinium, and Et_3NH^+) as the proton source. In 2008, Artero and co-workers employed related cobaloxime complexes with $Ru(bpy)_3^{2+}$, $[Ir(ppy)_2(bpy)]^{2+}$, and $ReBr(CO)_3(phen)$ to produce hydrogen photochemically,[33,34] but in these systems, the proton source was $[Et_3NH]BF_4$ or $[Et_3NH]Cl$ and not water. In fact, these systems encountered serious problems with low efficiency for hydrogen generation when water was added to the system.

In 2008, we extended our initial report of the photochemical generation of H_2 from aqueous protons and a sacrificial electron source in a system containing the Pt terpyridyl acetylide chromophore **C1** and a colloidal Pt catalyst to one having the same chromophore but with the Co dmg complex **1** as the molecular catalyst for H_2 formation.[35] In this paper, we present a much more detailed study of this system and expand our investigations to include other Co catalysts, different Pt sensitizers, variation of the solvent, and the effect of sacrificial donor and concentrations. The results lead to conclusions about different steps in the overall hydrogen-forming reaction and allow comparisons between different H_2-generating systems.

Experimental Section

Chemicals. Cobalt chloride hexahydrate, cobalt acetate tetrahydrate, dimethylglyoxime ($dmgH_2$), 4-(dimethylamino) pyridine (4-Me_2N-py), methyl isonicotinate (4-COOMe-py), and triethanolamine (TEOA) are commercially available (Aldrich) and were used as received. HPLC-grade acetonitrile (MeCN) was purchased from Fisher and used without further purification. The cobalt complexes $[Co(dmgH)_2pyCl]$ (**1**),[37] $[Co(dmgH)(dmgH_2)Cl_2]$ (**4**),[38] $[Co(dmgH)_2(py)_2](PF_6)$ (**5**),[39] $[Co(dmgBF_2)_2(OH_2)_2]$ (**7**),[40] $[Co(dmgH)_2(P(n\text{-}Bu)_3)Cl]$ (**6**),[41] and the platinum chromophores **C1**−**C7** (Scheme 3)[16,47] were synthesized as reported in the literature.

$[Co(dmgH)_2(4\text{-}COOMe\text{-}py)Cl]$ (2). A 500 mg (1.48 mmol) sample of $[Co(dmgH)(dmgH_2)Cl_2]$ was suspended in 50 mL of methanol. One equivalent of triethylamine was then added to the flask, after which the complex dissolved within 5 min, changing from a green suspension to a clear brown solution. Methyl isonicotinate, 203 mg (1.48 mmol), was then added and the solution stirred for 1 h following formation of a brown precipitate (10−20 min). The suspension was filtered and the precipitate washed with water (10 mL), ethanol (10 mL), and diethyl ether (10 mL) to give $[Co(dmgH)_2(4\text{-}COOMe\text{-}py)Cl]$ (**2**) (600 mg, 93%). ^1H NMR (400 MHz, $CDCl_3$): 8.40 (d, 2H, py), 7.70 (d, 2H, py), 3.87 (s, 3H, -COO*Me*), 2.35 (s, 12H, dmg^{2-}). Anal. calcd for $C_{15}H_{21}N_5ClCoO_6$: C, 39.02; H, 4.58; N, 15.17. Found: C, 38.88; H, 4.64; N, 15.02.

Characterization. ^1H NMR spectra were recorded on a Bruker Avance-400 spectrometer (400.1 MHz). Absorption spectra were recorded using a Hitachi U2000 scanning spectrophotometer (200−1100 nm). Luminescence spectra were obtained using a Spex Fluoromax-P fluorimeter corrected for the spectral sensitivity of the photomultiplier tube and the spectral output of the lamp with monochromators positioned for a 2 nm band-pass. Solution samples were degassed by three freeze−pump−thaw cycles.

Electrochemistry. Cyclic voltammetry experiments were conducted on an EG&G PAR 263A potentiostat/galvanostat using a three-electrode single-compartment cell including a glassy carbon working electrode, a Pt wire auxiliary electrode, and a Ag wire reference electrode. For all measurements, samples were degassed by bubbling argon through the solution for 10 min. Tetrabutylammonium hexafluorophosphate (Fluka) was used as the supporting electrolyte (0.1 M), and ferrocene was employed as an internal redox reference. All redox potentials were measured relative to the ferrocenium/ferrocene (Fc^+/Fc) couple (0.40 V vs SCE)[42] used as an internal standard and then adjusted to NHE (SCE vs NHE = 0.24 V). All scans were done at 100 mV s^{-1}.

Quenching Experiments. All quenching experiments were done by adding calibrated amounts of quencher into the chomophore solution at room temperature. The Pt chromophore solution was held fixed at 2.0×10^{-5} M in MeCN/water (3:2 v/v). The solutions were degassed through three freeze−pump−thaw cycles. Steady-state luminescence spectra were then collected for each sample. The relative emission intensity of the chromophore in the absence and presence of

(21) Bi, Z.; Qian, Y.; Huang, J.; Xiao, Z.; Yu, J. *J. Photochem. Photobiol. A: Chem.* **1994**, *77*, 37–40.
(22) Hashimoto, K.; Kawai, T.; Sakata, T. *Chem. Lett.* **1983**, *5*, 709–712.
(23) Hashimoto, K.; Kawai, T.; Sakata, T. *Nouv. J. Chem.* **1984**, *8*, 693–700.
(24) Islam, S. D. M.; Yoshikawa, Y.; Fujitsuka, M.; Ito, O.; Komatsu, S.; Usui, Y. *J. Photochem. Photobiol. A: Chem.* **2000**, *134*, 155–161.
(25) Jiang, D. L.; Choi, C. K.; Honda, K.; Li, W. S.; Yuzawa, T.; Aida, T. *J. Am. Chem. Soc.* **2004**, *126*, 12084–12089.
(26) Na, Y.; Pan, J.; Wang, M.; Sun, L. *Inorg. Chem.* **2007**, *46*, 3813–3815.
(27) Na, Y.; Wang, M.; Pan, J.; Zhang, P.; Åkermark, B.; Sun, L. *Inorg. Chem.* **2008**, 2805–2810.
(28) Razavet, M.; Artero, V.; Fontecave, M. *Inorg. Chem.* **2005**, *44*, 4786–4795.
(29) Baffert, C.; Artero, V.; Fontecave, M. *Inorg. Chem.* **2007**, *46*, 1817–1824.
(30) Hu, X.; Brunschwig, B. S.; Peters, J. C. *J. Am. Chem. Soc.* **2007**, *129*, 8988–8998.
(31) Hu, X. L.; Cossairt, B. M.; Brunschwig, B. S.; Lewis, N. S.; Peters, J. C. *Chem.Commun.* **2005**, 4723–4725.
(32) Brown, G. M.; Brunschwig, B. S.; Creutz, C.; Matsubara, T.; Sutin, N. *J. Am. Chem. Soc.* **1979**, *101*, 1298–1300.
(33) Fihri, A.; Artero, V.; Razavet, M.; Baffert, C.; Leibl, W.; Fontecave, M. *Angew. Chem., Int. Ed.* **2008**, *47*, 564–567.
(34) Fihri, A.; Artero, V.; Pereira, A.; Fontecave, M. *Dalton Trans.* **2008**, 5567–5569.
(35) Du, P. W.; Knowles, K.; Eisenberg, R. *J. Am. Chem. Soc.* **2008**, *130*, 12576–12577.
(36) Probst, B.; Kolano, C.; Hamm, P.; Alberto, R. *Inorg. Chem.* **2009**, *48*, 1836–1843.
(37) Schrauzer, G. N. *Inorg. Synth.* **1968**, *11*, 61.
(38) Trogler, W. C.; Stewart, R. C.; Epps, L. A.; Marzilli, L. G. *Inorg. Chem.* **1974**, *13*, 1564–1570.
(39) Gerli, A.; Marzilli, L. G. *Inorg. Chem.* **1992**, *31*, 1152–1160.
(40) Bakac, A.; Espenson, J. H. *J. Am. Chem. Soc.* **1984**, *106*, 5197–5202.
(41) Toscane, P. J.; Swider, T. F.; Marzilli, L. G.; Bresciani-Pahor, N.; Randaccio, L. *Inorg. Chem.* **1983**, *22*, 3416–3421.
(42) Connelly, N. G.; Geiger, W. E. *Chem. Rev.* **1996**, *96*, 877–910.

the quencher was used to calculate the quenching rate constant by the Stern−Volmer equation.[43]

Details of Hydrogen Production. For photoinduced hydrogen evolution, each sample was made in a 50 mL round-bottom flask with a volume of 25 mL in MeCN/water (3:2 v/v). Typically, the sample contained 1.1×10^{-5} M Pt chromophore, 1.6×10^{-2} M TEOA, and 2.0×10^{-4} M cobaloximes. The flask was sealed with a septum and degassed by bubbling nitrogen for 15 min under atmospheric pressure at room temperature. After that, 5 mL of nitrogen was removed from the flask and 5 mL of methane (760 Torr) was added to the flask to serve as the internal standard for gas chromatography (GC) measurements. The samples were irradiated by a 200W Mercury Xeon lamp with a filter that cut off light with $\lambda < 410$ nm. The quantities of hydrogen were measured by GC using a Shimadzu GC-17A chromatograph with a Molecular Sieve 5Å column (30 m × 0.53 mm).

X-Ray Structural Determination of Complexes 2 and 3. Brown crystals of **2** and red crystals of **3** suitable for single-crystal X-ray diffraction were maintained at 100.0(1) K, on a Bruker SMART platform diffractometer equipped with an APEX II CCD detector. The X-ray source, powered at 50 kV and 30 mA, provided Mo Kα radiation ($\lambda = 0.71073$ Å, graphite monochromator). Space groups were determined based on systematic absences, intensity statistics, and space group frequencies. Direct methods were used to solve the structures.[44] Full-matrix least-squares/difference Fourier cycles were performed, which located the remaining non-hydrogen atoms. All non-hydrogen atoms were refined with anisotropic displacement parameters. All hydrogen atoms were given riding models and refined with relative isotropic displacement parameters.

Results and Discussion

Synthesis and Electronic Absorption. Cobaloxime complexes **2** and **3** were synthesized by stirring a 1:1 ratio of $Co(dmgH)(dmgH_2)Cl_2$ and the corresponding pyridine derivative in methanol.[38] One of the chloride ligands in $Co(dmgH)(dmgH_2)Cl_2$ was replaced by the corresponding pyridine derivative to form **2** and **3** with yields of over 85% (Scheme 1).

The UV−vis absorption spectra of complexes **1**−**7** (see Scheme 2 for complexes) measured at room temperature in MeCN/water (3:2 v/v) are shown in Figure 1. Complexes **1**−**6** exhibit a broad high-energy absorption between 220 and 300 nm with ε on the order of 10^4 dm^3 mol^{-1} cm^{-1}, which corresponds to spin-allowed intraligand ($\pi-\pi^*$) transitions. Unlike the Co(III) complexes **1**−**6**, catalyst **7** possesses a very different absorption spectrum with a broad low-energy band between 400 and 530 nm centered at 442 nm ($\varepsilon \sim 7750$ dm^3 mol^{-1} cm^{-1}) corresponding to Co(II) absorption, as assigned previously.[30,40]

Structural Characterization of Complexes 2 and 3. The solid-state molecular structures of **2** and **3**, as determined by single-crystal X-ray crystallography, are shown in Figure 2 with important crystallographic parameters and bond lengths and angles given in Tables 1 and 2, respectively. In both **2** and **3**, the refined structure reveals a six-coordinate Co(III) ion that is ligated by two coplanar dimethylglyoximate ligands and trans chloride

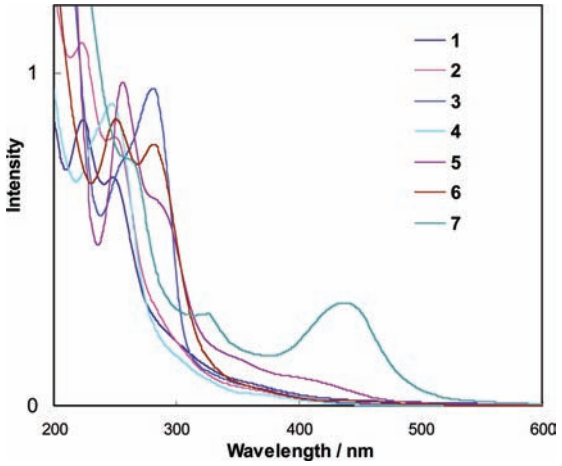

Figure 1. Normalized absorption spectra of cobaloxime complexes **1**−**7** in MeCN/water (3:2 v/v) at 4.0×10^{-5} M.

Scheme 1

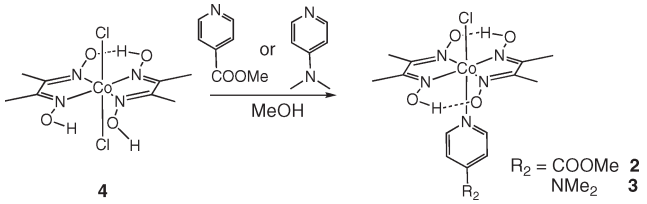

Scheme 2

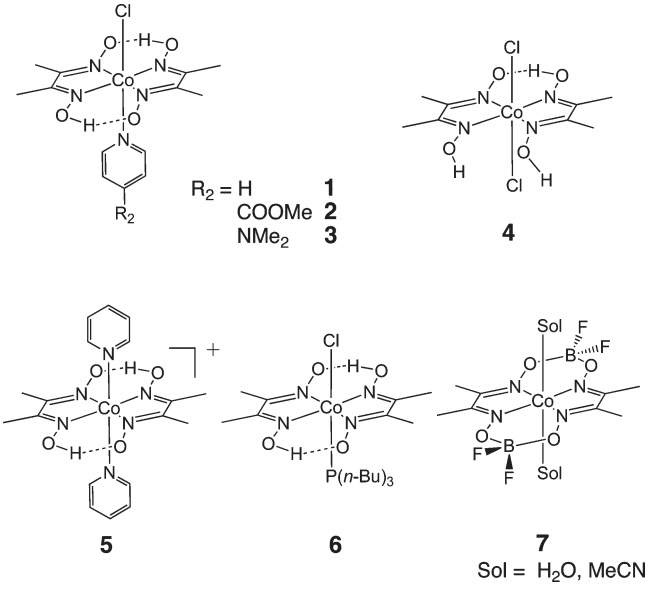

and pyridine ligands. The observed axial $Co-N_{pyridine}$ distances of 1.959 Å in complex **2** and 1.946 Å in complex **3** agree closely with those of in other Co(III) cobaloximate complexes, such as $[Co(dmgH)_2pyCl]$ with a $Co-N_{pyridine}$ distance of 1.959 Å.[45] The average $Co-N_{imine}$ bond distances of the glyoximate ligands in **2** and **3** are 1.892 and 1.891 Å, respectively, which are consistent with the values of 1.895 Å in $[Co(dmgH)_2pyCl]$,[45] 1.891 Å in

(43) Vincze, L.; Sandor, F.; Pem, J.; Bosnyak, G. *J. Photochem. Photobiol.* **1999**, *120*, 11–14.
(44) *SHELXTL*, V.6.14; Bruker AXS: Madison, WI, 2000.
(45) Geremia, S.; Dreos, R.; Randaccio, L.; Tauzher, G. *Inorg. Chim. Acta* **1994**, *216*, 125–129.

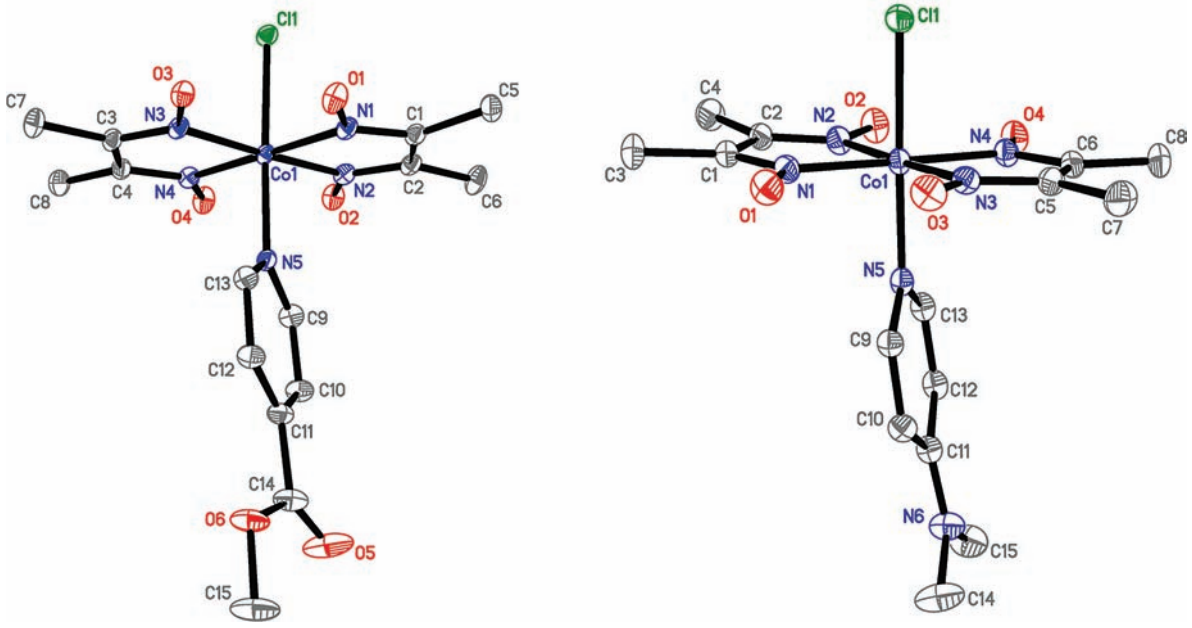

Figure 2. Perspective views of complex **2** (left) and complex **3** (right) with atomic numbering scheme. All hydrogen atoms have been omitted for clarity.

Table 1. Crystallographic, Data Collection, and Structure Refinement Parameters for Complexes **2** and **3**

form	brown needle (complex **2**)	red prism (complex **3**)
empirical formula	$C_{17}H_{27}ClCoN_5O_7$	$C_{15}H_{24}ClCoN_6O_4$
fw	507.82	446.78
T, K	100.0(1)	100.0(1)
wavelength, Å	0.71073 Å	0.71073 A
cryst syst	monoclinic	monoclinic
space group	$P2_1/c$	$P2_1/n$
Z	4	4
a, Å	9.9436(7)	7.886 (2)
b, Å	22.955(2)	22.361(5)
c, Å	9.6917(6)	13.229(3)
α, β, γ, deg	90°, 91.317(1)°, 90°	90°, 92.98(3)°, 90°
V, Å^3	2211.6(3)	2329.7(8)
ρ_{calcd}, Mg/m^3	1.525	1.274
μ, mm^{-1}	0.945	0.880
cryst size, mm^3	0.24 × 0.20 × 0.04	0.32 × 0.14 × 0.12
F(000)	1056	928
2θ range, deg	2.05 to 34.97°	1.79 to 26.00°
limiting indicies	$-16 \le h \le +16$, $-37 \le k \le +37$, $-15 \le l \le +15$	$-9 \le h \le +9$, $-27 \le k \le +27$, $-16 \le l \le +16$
no. of reflns collected	35749	26914
no. of data/restraints /params	9578/3/303	4580/0/244
goodness of fit[a]	1.016	1.073
R1, wR2 ($l > 2\sigma$)[b]	R1 = 0.0514, wR2 = 0.1007	R1 = 0.0349, wR2 = 0.0976
R1, wR2 (all data)[b]	R1 = 0.0964, wR2 = 0.1165	R1 = 0.0380, wR2 = 0.0992

[a] GOF = $[\sum[w(F_o^2 - F_c^2)^2]/(m-n)]^{1/2}$, where n and p denote the number of data and parameters. [b] $R1 = \sum||F_o| - |F_c||/\sum|F_o|$ and wR2 = $[\sum[w(F_o^2 - F_c^2)^2]/\sum[w(F_o^2)^2]]^{1/2}$), where $w = 1/[\sigma^2(F_o^2 + (aP)^2 + bP]$ and $P = 1/3 \max(0, F_o^2) + 2/3F_c^2$.

$[Co(dmgH)_2(4\text{-CN-py})Cl]$,[46] and 1.891 Å in $[Co(dmgH)_2(2,6\text{-dimethylpyrazine})Cl]$.[46]

Electrochemistry of Cobaloximes. Cyclic voltammetry studies were performed on all of the complexes in MeCN with 0.1 M tetra-*n*-butylammonium hexafluorophosphate as the supporting electrolyte under an argon atmosphere. All of the redox potentials were measured and adjusted to NHE using the ferrocenium/ferrocene (Fc^+/Fc) couple as an internal standard and then adjusting the potentials using literature values for the internal standard (0.40 V vs SCE, SCE vs NHE = 0.24 V).[42] All cobaloxime complexes in the present study exhibit the expected number of reductions and oxidations, and the results are summarized in Table 3. The redox potentials were also compared with values measured in DMF solution and found to have slight but significant differences.[28] For example, complex **1** in MeCN shows one irreversible reduction assigned to a Co(III)/Co(II) process at −0.43 V versus NHE, followed by a reversible reduction of Co(II) to Co(I) at −0.88 V, whereas in DMF the same complex exhibits the first and second reduction potentials at −0.37 and −0.76 V, corresponding to a slight anodic shift. Complex **1** also shows an irreversible oxidation

(46) Concepcion Lopez, S. A.; Xavier Solans, M. F. *Inorg. Chem.* **1986**, *25*, 2962–2969.

Table 2. Selected Bond Lengths (Å) and Angles (deg) for Complexes **2** and **3**

Complex 2

bond lengths		bond angles	
Co(1)−N(2)	1.884(2)	N(2)−Co(1)−N(1)	81.90(7)
Co(1)−N(1)	1.889(2)	N(2)−Co(1)−N(3)	177.08(7)
Co(1)−N(3)	1.895(2)	N(1)−Co(1)−N(3)	98.97(7)
Co(1)−N(4)	1.900(2)	N(2)−Co(1)−N(4)	97.81(7)
Co(1)−N(5)	1.959(2)	N(1)−Co(1)−N(4)	179.44(7)
Co(1)−Cl(1)	2.2279(5)	N(3)−Co(1)−N(4)	81.30(7)
N(1)−O(1)	1.347(2)	N(2)−Co(1)−N(5)	91.06(7)
N(2)−O(2)	1.339(2)	N(1)−Co(1)−N(5)	89.02(7)
N(3)−O(3)	1.344(2)	N(3)−Co(1)−N(5)	91.73(7)
N(4)−O(4)	1.345(2)	N(4)−Co(1)−N(5)	91.47(7)

Complex 3

bond lengths		bond angles	
Co(1)−N(3)	1.8831(9)	N(3)−Co(1)−N(4)	81.68(4)
Co(1)−N(4)	1.8908(9)	N(3)−Co(1)−N(1)	98.61(4)
Co(1)−N(1)	1.8945(9)	N(4)−Co(1)−N(1)	179.24(4)
Co(1)−N(2)	1.8976(9)	N(3)−Co(1)−N(2)	177.96(4)
Co(1)−N(5)	1.9464(9)	N(4)−Co(1)−N(2)	98.31(4)
Co(1)−Cl(1)	2.2364(3)	N(1)−Co(1)−N(2)	81.36(4)
N(1)−O(1)	1.346(1)	N(3)−Co(1)−N(5)	89.54(4)
N(2)−O(2)	1.341(1)	N(4)−Co(1)−N(5)	89.07(4)
N(3)−O(3)	1.331(1)	N(1)−Co(1)−N(5)	91.63(4)
N(4)−O(4)	1.344(1)	N(2)−Co(1)−N(5)	92.50(4)

process at +1.37 V (vs NHE) in MeCN, attributable to a Co(III)/Co(IV) process. All of the other cobalt complexes except **7** have the same trend in reduction potentials between MeCN and DMF, with the latter being slightly less negative, 0.01−0.15 V. In contrast, for the $dmgBF_2$ complex **7**, the reduction wave of the Co(II)/Co(I) couple in MeCN, −0.29 V versus NHE, is slightly more positive than the corresponding potential in DMF.[29,30]

Quenching Studies and Photoreduction of Co Complexes 1−7. Complexes **1**−**7** were all observed to quench the luminescence of the Pt chromophore **C1**. In all samples, quenching constants (k_q) were determined using the Stern−Volmer equation (eq 1),[43] where I_0 is the integrated metal-to-ligand charge-transfer emission intensity in the absence of a quencher, I is the corresponding value in the presence of a quencher, τ_0 is the excited-state lifetime in the absence of a quencher (for **C1**, τ_0 = 4.6 μs[16]), k_q is the bimolecular quenching rate constant, and [Q] is the molar concentration of the quencher.

$$I_0/I = 1 + k_q\tau[\mathrm{Q}] \qquad (1)$$

All of the cobaloxime complexes except **5** give fast quenching rates close to the diffusion-controlled limit of $\sim 1 \times 10^{10}$ M^{-1} s^{-1}. Among these complexes, **2** yields the fastest quenching rate at 1.7×10^9 M^{-1} s^{-1}. It is noteworthy that complex **5** has a quenching rate constant 2 orders of magnitude slower than the other cobaloximes. While the reason for this difference was not investigated, it could relate to the fact that **5** is the only complex that does not have a chloride ligand for possible interaction with the Pt chromophore in the quenching process.

In the photolysis solutions containing **C1**, TEOA, and complex **1**, the bright yellow color of Co(II) develops within 10 min and continues to increase in intensity up to a limiting value after ca. 50 min.[35] When irradiation is stopped, the bright yellow color persists under an inert atmosphere but dissipates upon exposure of the solution to air within 1−2 min. For the other cobaloximes (**2**−**4**, **6**), similar quenching behavior in the presence of TEOA is also observed.

When complex **7**, which contains Co(II), serves as the electron acceptor, quenching is also observed with a decrease in the photoluminescence of **C1**, and in the presence of TEOA, the formation of a persistent blue color with maxima at 550 and 650 nm (Figure 3) that is characteristic of the corresponding Co(I) absorption[30] is seen. UV−vis spectra show an isosbestic point at 465 nm, indicating no decomposition during the Co(II) reduction.

Hydrogen Production. A series of experiments using complexes **1**−**7** for hydrogen production have been carried out employing visible light irradiation ($\lambda > 410$ nm) and the following concentrations and conditions: 1.1×10^{-5} M Pt chromophore, 1.6×10^{-2} M TEOA, and 2.0×10^{-4} M cobaloxime complex catalyst in MeCN/water (3:2 v/v). Quantitative determination of generated H_2 was conducted by GC analysis with added methane as an internal standard, as described in the Experimental Section. During initial observations using complex **1**, the pH of the reaction solution was varied between 5 and 13, and both the rate and the amount of H_2 generated was seen to maximize at pH ~8.5. Below pH 5, no H_2 generation was observed, and above pH 12, the amounts of H_2 produced were moderate (less than 15% of that obtained at pH 8.5 during the same amount of irradiation).

Table 4 shows the results of these photolytic hydrogen production experiments. No hydrogen can be detected in the absence of any cobaloxime complex (run 9), indicating that the cobalt catalyst is one of the key components of the homogeneous hydrogen production system. Complex **2** proved to be the most active of the cobaloximes examined, with up to 238 turnovers of H_2 obtained after 5 h of irradiation (run 2), while further photolysis led to increased hydrogen yields (run 3).

For complex **6**, in which the axial pyridine of **1** is replaced by P(*n*-Bu)$_3$, no hydrogen was evolved in 5 h of photolysis (run 7), despite the fact that the redox potential of the Co(II)/Co(I) couple (−0.74 V vs NHE in MeCN) is thermodynamically favorable for proton reduction. It has been reported that **6** undergoes reaction with $NaBH_4$ to form the stable Co(III) hydride [CoH(dmgH)$_2$(P(*n*-Bu)$_3$)] that yields hydrogen only upon thermolysis at 150 °C.[49] It is therefore possible to ascribe the poor catalytic activity of **6** for H_2 generation in the present study to the great stability of [CoH(dmgH)$_2$(P(*n*-Bu)$_3$)], as compared with analogous hydride complexes [CoH(dmgH)$_2$py] having pyridine ligands trans to the hydride that are much less stable.[49]

In the context of H_2 evolution, the Co(II) complex **7**, [Co(dmgBF$_2$)$_2$(OH$_2$)$_2$], which possesses good air and acid stability, was studied initially by Espenson and Connolly.[50]

(47) Schneider, J.; Du, P.; Jarosz, P.; Lazarides, T.; Wang, X.; Brennessel, W. W.; Eisenberg, R. *Inorg. Chem.* **2009**, in press.

(48) Cline, E. D.; Adamson, S. E.; Bernhard, S. *Inorg. Chem.* **2008**, *47*, 10378–10388.

(49) Schrauzer, G. N.; Holland, R. J. *J. Am. Chem. Soc.* **1971**, *93*, 1505–1506.

(50) Connolly, P.; Espenson, J. H. *Inorg. Chem.* **1986**, *25*, 2684–2688.

Table 3. Electrochemical Potentials[a] (V, vs NHE) for Cobaloximes and **C1**.

Compound	Oxidation[b]	Reduction[c] $E_{1/2}$/v		Reduction[d] $E_{1/2}$/v		k_q[e] $M^{-1}s^{-1}$
$[Co(dmgH)_2(py)Cl]$	1.37	−0.43	−0.88	−0.37	−0.76	1.3×10^9
$[Co(dmgH)_2(4\text{-}COOMe\text{-}py)Cl]$	1.39	−0.53	−0.84			1.7×10^9
$[Co(dmgH)_2(4\text{-}Me_2N\text{-}py)Cl]$	1.33	−0.59	−0.88	−0.44	−0.79	1.2×10^9
$[Co(dmgH)(py)_2](PF_6)$	1.64	−0.14	−0.85	−0.02	−0.76	4.0×10^7
$[Co(dmgBF_2)_2(OH_2)_2]$	1.23		−0.29		−0.33	1.3×10^9
$[Co(dmgH)_2Cl_2]$	1.54	−0.24	−0.55			1.0×10^9
$[Co(dmgH)_2(P(n\text{-}Bu)_3)Cl]$	1.35	−0.67	−0.74	−0.40	−0.59	1.6×10^9
$[Pt(ttpy)(phenylacetylide)]^+$	1.56	−0.68	−1.16	−0.59	−1.07	

[a] Electrochemical data were obtained in degassed solution with 0.1 M n-Bu_4NPF_6 (TBAH) as supporting eletrolyte at room temprature; Scan Rate:100 mV/sec; potential vs NHE converted from internal standard $Fc^{+/0}$ using Ref.[42]; [b] Irreversible oxidation peak estimated vs NHE in MeCN solution with $Fc^{+/0}$ as an internal standard; [c] Reversible reductions measured in MeCN solution with $Fc^{+/0}$ as an internal standard and adjusted to vs NHE; [d] Reductions measured in DMF solution and adjusted to vs NHE. Taken from Ref. [28]; [e] Measured in MeCN/water (3:2 v/v); [f] The excited state *oxidation* potential (vs NHE) of $[Pt(ttpy)(phenylacetylide)]^+$ (**C1**) has been estimated as −0.92 V (when written conventionally as a reduction).[17]

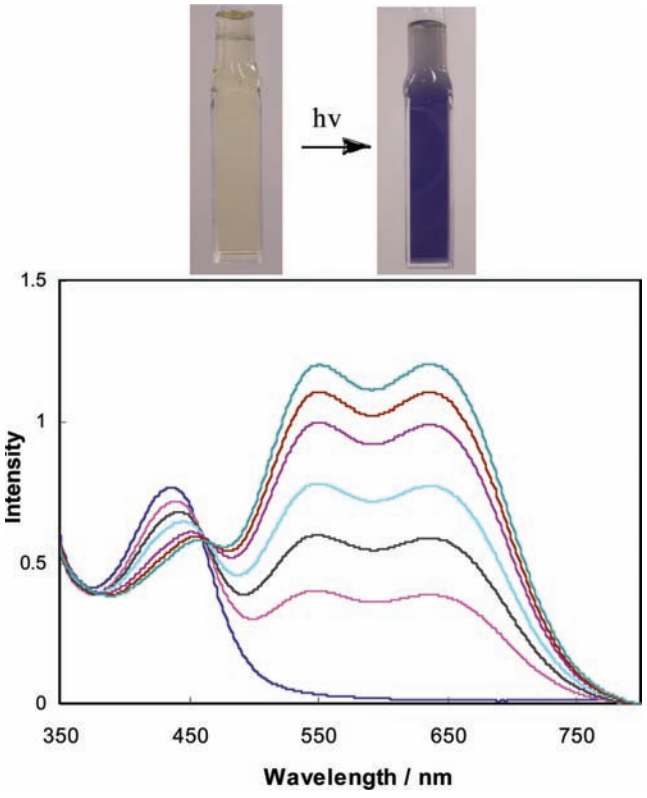

Figure 3. Formation of Co(I) upon visible light irradiation of a solution containing 1.1×10^{-5} M Pt chromophore **C1**, 1.6×10^{-2} M TEOA, and 2.0×10^{-5} M complex **7** ($[Co(dmgBF_2)_2(OH_2)_2]$).

The generation of H_2 was the result of the chromous ion reduction of **7** and thus became catalytic in Co(II). Within the past decade, the chemistry of this complex has been revisited for catalysis of H_2 generation, and it has been found to have excellent activity for *electro*catalytic hydrogen production in nonaqueous media.[28,30] Accordingly, we examined this complex in the present *photo*chemical system for hydrogen production (run 8). Despite its advantages for *electro*chemical proton reduction in terms of low overpotential for H_2 evolution, the complex did not function satisfactorily as a catalyst in the current photochemical system for hydrogen production. In this run, the system pH was set to 8.5, at which value the H^+ reduction potential is ca. −0.48 V, which is negative relative to the Co(II)/Co(I) couple (−0.29 V vs NHE, Table 3). While not rigorously correct from a thermodynamic point of view because of differences in the *media* of the quoted potentials, the results strongly suggest that complex **7** is not thermodynamically able to act as a proton reduction catalyst at this pH. An analogous system containing $Ru(bpy)_3^{2+}$ as the photosensitizer with $[Co(dmgBF_2)_2(MeCN)_2]$ as the catalyst and ascorbic acid as the sacrificial donor at pH = 2.0 was examined by us, and while it did yield hydrogen, it did so in only very small amounts. A slightly different result was obtained by Artero and co-workers in nonaqueous media with a system composed of $Ru(bpy)_3^{2+}$, $Co(dmgBF_2)_2$, and $[Et_3NH]Cl$ as the proton source that yielded 20 TNs of H_2 formation under UV irradiation but much less under visible light irradiation.[33]

Table 4. Photocatalytic Hydrogen Production Using Different Cobaloximes as the Catalysts[a]

run	complex	irrad. time/h	TNs
1	**1**	5	193
2	**2**	5	238
3	**2**	10	378
4	**3**	5	106
5	**4**	5	124
6	**5**	5	125
7	**6**	5	< 1
8	**7**	5	< 1
9		5	< 1
10[b]	**1**	5	< 1
11[c]	**1**	5	25
12[d]	**1**	5	56
13[e]	**1**	5	92

[a] General conditions: The reaction was run in MeCN/water (3:2 v/v) at pH = 8.5 in the presence of 1.6×10^{-2} M TEOA, 1.1×10^{-5} M photosensitizer **C1**, and 2.0×10^{-4} M cobaloximes. [b] In DMSO/water (3:2 v/v). [c] In DMF/water (3:2 v/v). [d] In MeOH/water (3:2 v/v). [e] In EtOH/water (3:2 v/v).

In all of the hydrogen production experiments that yielded H_2, induction periods were observed. Typically, hydrogen evolution commenced only after 1−2 h of irradiation of the sample. The observed induction periods are consistent with the notion that Co(III) must first be converted into Co(II) and then Co(I) for the photogeneration of H_2 to occur.[35] This hypothesis is supported by UV−vis spectroscopic monitoring of the reaction system as a function of time.

Solvent variation has a substantial effect on the rate and amount of hydrogen production. Smaller quantities of hydrogen were produced in systems having a different

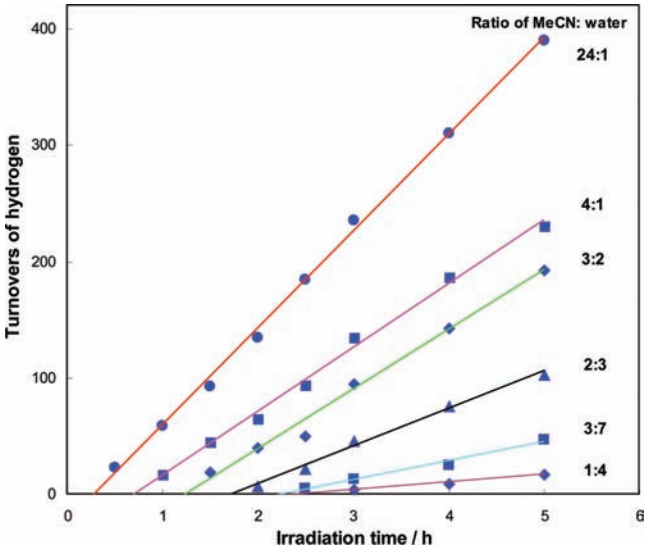

Figure 4. Comparison of hydrogen production using different ratios of MeCN/water with 1.1×10^{-5} M Pt chromophore **C1**, 1.6×10^{-2} M TEOA, and 2.0×10^{-5} M complex **1** at pH = 8.5.

organic solvent, albeit with the same 3:2 v/v ratio with water, for example, in DMSO (Table 4, run 10, no appreciable H_2 was seen within 5 h), in DMF (run 11, 25 TNs were obtained within 5 h), in MeOH (run 12, 56 TNs within 5 h), and in EtOH (run 13, 92 TNs within 5 h). The solvent dependence for hydrogen evolution from this system probably results from a number of factors including solvent polarity, stabilization of reduction intermediates, solvent coordination ability for binding to Co, the driving force dependence for the ultimate H_2 generation reaction (as discussed below, either the Co(II)/Co(I) couple or reduction of a Co(III) hydride intermediate), and catalyst stability.

Further studies on medium effects were done to investigate the catalytic activity of the photochemical hydrogen reaction by changing the ratio of MeCN and water. The results are shown in Figure 4, demonstrating that the photochemical reaction has a higher rate of hydrogen production when the ratio of MeCN/water is increased. When the MeCN/H_2O ratio is increased to 24:1 from 3:2, the rate of H_2 generation essentially doubles, with H_2 TNs growing to 390 from 193 after 5 h of irradiation. The induction time for producing hydrogen is also shortened at higher MeCN concentrations, decreasing from 80 to 15 min when the MeCN/H_2O ratio changes from 3:2 to 24:1. The effect of the MeCN/H_2O ratio may be attributable to differences in the reduction potentials in different media[51] *or* a change in solvent dielectric constant as the MeCN/H_2O ratio changes (the solvent dielectric constants for MeCN and H_2O are 36.6 and 80, respectively).[48]

There is no significant trend in the potentials for the Co(II)/Co(I) couple between complexes **1**−**3** in which the axial pyridine ligand is modified in the 4- position to possess either an electron-donating group (−NMe_2) as in **3** or an electron-withdrawing group (−COOMe) as in **2**, an observation in accord with earlier work on

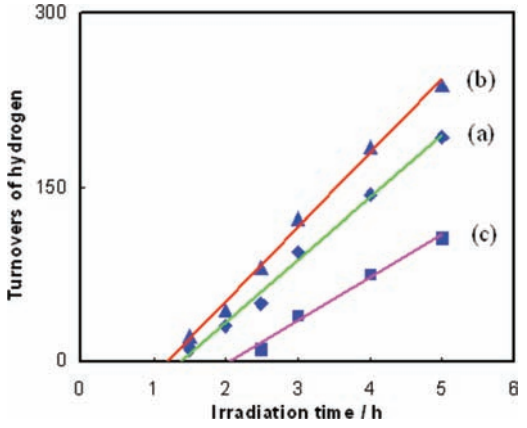

Figure 5. Comparison of hydrogen production using different cobaloximes with 1.1×10^{-5} M Pt chromophore **C1**, 1.6×10^{-2} M TEOA, and 2.0×10^{-5} M catalyst at pH = 8.5. (a) Complex **1**; (b) complex **2**; (c) complex **3**.

alkyl cobaloximes.[52] Interestingly, however, these three complexes, **1**−**3**, exhibit different activities for hydrogen production, as shown in Figure 5. Complex **2** with the electron-withdrawing axial ligand (4-MeOOC-py) is more active than complex **1** (Table 4, run 1), while **3** with the more electron-donating pyridine (4-Me_2N-py; Table 4, run 4) is less active than **1**. With regard to the induction period, the plot (Figure 5) shows that hydrogen generation commences following the same order as the activity: **2** > **1** > **3**. This ordering is also in accord with modest changes in the quenching rate constants (**2** > **1** > **3**), consistent with the importance of electron transfer from the excited chromophore to the Co catalyst despite the absence of a correlation in the Co reduction potentials.

In a study of the effects of axial pyridine substituents on H_2 production via *electro*catalysis, Artero et al. found that the largest rates of H_2 production were obtained with cobaloximes that possessed electron-donating axial pyridines, in contrast with the present results.[28] This difference in activity may be a consequence of the different media and optimal pH ranges employed in the two studies.

Complexes **4** and **5** were also examined as the potential hydrogen catalysts. Both complexes have the same D_{2h} symmetry with trans Cl^- ligands for **4** and trans pyridine ligands for **5**. These two complexes showed different reactivity for hydrogen production, as shown in Figure 6. While complex **4** did produce hydrogen after 1 h of irradiation, the plot of H_2 production versus time leveled off after 4 h, indicating instability of the catalyst complex during photolysis. For complex **5**, hydrogen production exhibited a linear relationship with the irradiation time even after 6 h of photolysis, but **5** yielded a slower rate of hydrogen production than **1**, possibly because of its slow oxidative quenching rate constant with photoexcited **C1** (Table 3, $k_q = 4.0 \times 10^7$ M^{-1} s^{-1}).

In the initial report of the photochemical production of H_2 using **1** as the hydrogen-generating catalyst, [Pt(ttpy)(C≡CPh)]ClO_4 (**C1**) was employed as the light-harvesting chromophore.[35] In the present study, the related chromophores **C2**−**C4** (Scheme 3) were examined as to their effectiveness under similar experimental conditions: $\lambda >$ 410 nm; Pt(II) chromophore, 1.1×10^{-5} M; TEOA, 1.6×10^{-2} M; Co complex **1**, 2.0×10^{-4} M in MeCN/water (3:2 v/v), pH = 8.5. Figure 7A shows the time dependence

(51) Abe, R.; Sayama, K.; Sugihara, H. *J. Sol. Energy Eng.* **2005**, *127* 413–416.
(52) Schrauzer, G. N.; Windgassen, R. J. *J. Am. Chem. Soc.* **1966**, *88*, 3738–3743.

of hydrogen production in this reaction system for the different Pt chromophores. The plot demonstrates that the rate of hydrogen generation follows the order **C4** > **C2** > **C3** > **C1**, which is dependent on both the absorptivities of the chromophores and their quenching rate constants with Co complex **1**, as has been discussed previously.[17] The differences between the induction periods in Figure 7 relate to the effectiveness of the reduction of Co(III) to Co(II) and then to Co(I) before the onset of H_2 generation, as well as to instrument sensitivity at low H_2 levels.

Interestingly, H_2 was also observed when Pt(II) terpyridyl acetylide complexes were replaced by the cyclometalated Pt(II) acetylide complexes Pt(C^N^N−Ph−R)(C≡CPh) where R = Me (**C5**), COOMe (**C6**), and P(O)$(OEt)_2$ (**C7**) (Scheme 3). The experiments were run under the same reaction conditions as used for **C1**−**C4**, and the results are given in Figure 7B. The photochemical activity of **C5** is comparable with that of **C1**, yielding 170 TNs in 5 h. Within the same photolysis time, systems containing **C6** and **C7** generate 90 TNs and 120 TNs, respectively, which are less efficient than **C5**. While the luminescence of **C5**−**C7** is not readily quenched by the sacrificial donor (TEOA), oxidative quenching of the excited states of **C5**−**C7** by the Co catalyst complexes indeed occurs, and this is likely be the first step toward H_2 production. Oxidative quenching was established in separate experiments involving Co complex **1** with the cyclometalated chromophores **C5**−**C7** and yielded near diffusion-controlled quenching rate constants k_q of 3.6×10^9 M^{-1} s^{-1}, 2.9×10^9 M^{-1} s^{-1} and 2.1×10^9 M^{-1} s^{-1}, respectively. In the presence of both a reductive quencher (TEOA) and complex **1**, visible light excitation of the C^N^N chromophores generated a yellow color characteristic of Co (II) species, as seen in similar experiments with the Pt(II) terpyridyl acetylide chromophores and confirmed by UV−vis spectroscopy.

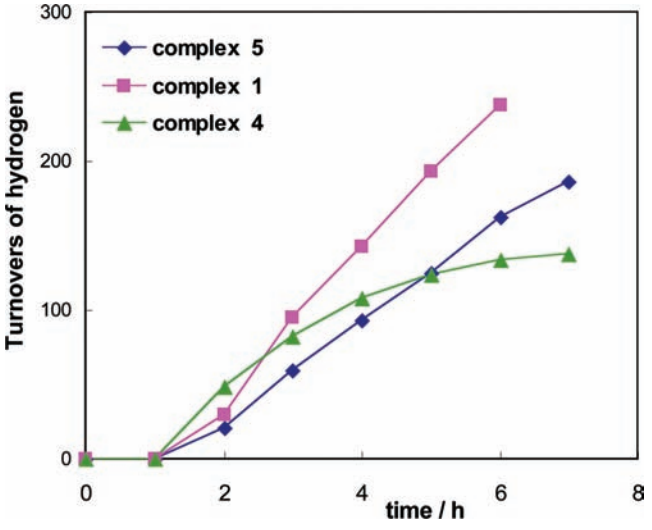

Figure 6. Comparison of hydrogen production using different cobaloximes **1**, **4**, and **5** under the following conditions: 1.1×10^{-5} M Pt chromophore **C1**, 1.6×10^{-2} M TEOA, and 2.0×10^{-5} M cobaloxime at pH = 8.5.

Examination of the influence of the TEOA concentration on the rate of H_2 production was examined by the runs shown in Figure 8. Only the concentration of TEOA is changed between these runs, with all other concentrations and conditions kept the same: λ > 410 nm; chromophore **C1**, 1.1×10^{-5} M; Co complex **1**, 2.0×10^{-4} M in MeCN/water (3:2 v/v), pH = 8.5. When the TEOA concentration was 6.7 mM, photolysis led to only 63 TNs, while in the presence of a TEOA concentration of 134 mM, 500 TNs were achieved with a yield of 21% based on TEOA in 5 h. With a further increase in TEOA concentration to 0.27 M, ~1000 turnovers were obtained after 10 h of irradiation. Along with greater yields of H_2 generation as [TEOA] is increased, the induction period for H_2 generation was also reduced. An explanation for increased turnovers of H_2 and decreased induction periods with greater concentrations of TEOA is most likely related to faster reductive quenching that also leads to a more rapid rate of transferring the second electron from the decomposing $TEOA^{+\bullet}$ radical cation.

A further investigation of the effect of [TEOA] was also conducted in the systems for which the ratio of MeCN/H_2O was 24:1. As above, both the rate of hydrogen production and the induction period were positively affected by increasing TEOA concentrations. The H_2 production system gave 390, 432, and 575 turnovers in 5 h as [TEOA] was varied from 16.1 to 47.5 and 134 mM, respectively. With a TEOA concentration of 0.27 M, ~2150 turnovers were obtained after 10 h of irradiation, giving an average rate of hydrogen production of ~215 turnovers per hour.

The Mechanism of Cobalt Species in Hydrogen Production. The mechanism of the visible-light-driven formation of hydrogen in the system containing the Pt chromophore **C1** and the cobaloxime catalyst **1** has been briefly discussed before.[35] The production of hydrogen involves

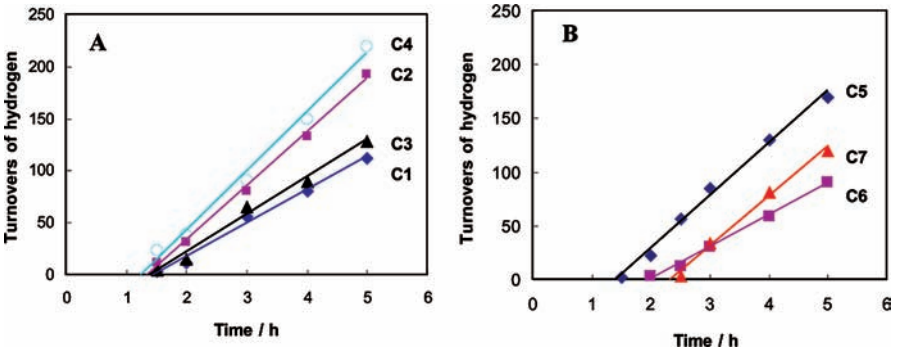

Figure 7. Hydrogen production using different Pt(II) chromophores under the following conditions: 1.1×10^{-5} M Pt chromophore, 1.6×10^{-2} M TEOA, and 2.0×10^{-5} M complex **1** at pH = 8.5. (A) Pt(II) terpyridyl acetylide chromophores; (B) cyclometalated Pt(II) acetylide chromophores.

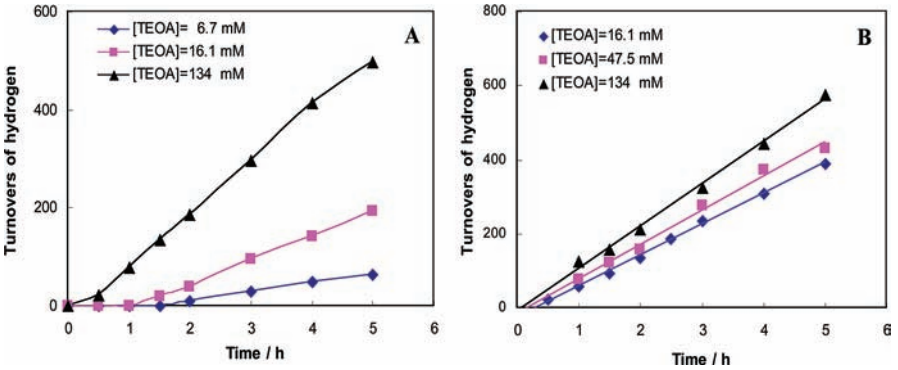

Figure 8. (A) Comparison of hydrogen production under different concentrations of TEOA (together with 1.1×10^{-5} M Pt chromophore **C1** and 2.0×10^{-5} M complex **1** at pH = 8.5). (B) Comparison of hydrogen production under a higher ratio of MeCN/water (v/v 24:1; together with 1.1×10^{-5} M Pt chromophore **C1** and 2.0×10^{-5} M complex **1** at pH = 8.5).

Scheme 3

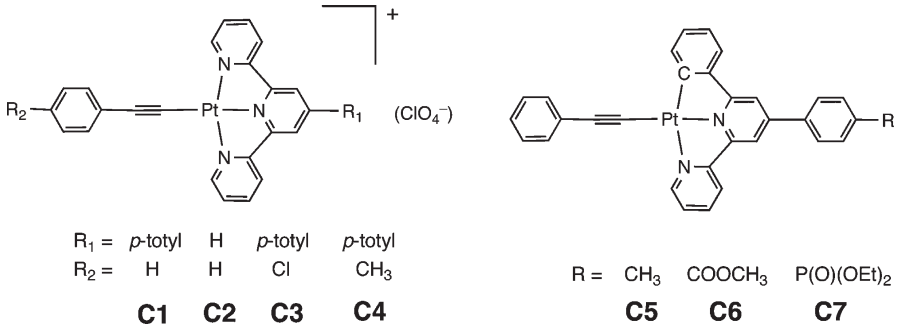

two irreversible processes—decomposition of the TEOA sacrificial donor and the release of hydrogen—and two reversible cycles—a photochemical Pt cycle and a catalytic Co cycle. The photochemical cycle can proceed along two paths, one based on reductive quenching and the other on oxidative quenching of the photoexcited chromophore. In the reductive quenching pathway, the excited chromophore **C1*** will be quenched by TEOA to form $\mathbf{C1}^-$ and $TEOA^+$, after which $TEOA^+$ loses a proton and another electron on its decomposition path to glycolaldehyde and di(ethanol)amine. Electron transfer from $\mathbf{C1}^-$ to Co(III) occurs, to regenerate the ground-state chromophore **C1**. For the oxidative quenching process, the Co complex serves as an electron acceptor to quench excited **C1*** to give $\mathbf{C1}^+$ and Co(II). The TEOA sacrificial donor will then be oxidized by $\mathbf{C1}^+$, leading to regeneration of the ground state of **C1**.

The catalytic cobalt cycle begins with reduction of the catalyst in one-electron steps to Co(I), followed by protonation of the cobaloxime anion to give a Co(III) hydride intermediate. Spectroscopic study of the system **C1** + **1** + TEOA shows that, prior to H_2 formation, stepwise reduction to Co(II) and Co(I) occurs (the latter is seen directly at pH 12, at which only very small amounts of H_2 are generated). During photolysis, in which H_2 is generated, the resting state of the system is Co(II).[35] These observations are entirely consistent with the previously reported work by Espenson and Connolly,[50] Artero and co-workers,[28,29] and Peters and co-workers.[30,31] Subsequent reaction of the Co(III) hydride formed by protonation of Co(I) represents a branch point in the mechanistic proposals for the generation of H_2. In one proposal, the Co(III) hydride reacts with H^+ to give H_2 and Co(III), which is subsequently reduced. An alternative single Co mechanism involves reduction of the Co(III) hydride to yield Co(II)−H that subsequently reacts with H^+ to form H_2 + Co(II). A kinetically distinguishable proposal for H_2 formation that has been put forth by others involves the reaction of two Co(III) hydrides to give H_2 + 2 Co(II).[28−31,50]

To address the kinetic dependence of the Co catalyst in the photochemical system studied here, a series of photolyses were run in which the cobalt catalyst concentration [Co] was varied while all other reaction parameters were held fixed and the TEOA concentration remained nearly constant. Complex **1** was used as the hydrogen-evolving catalyst for these experiments. The results are shown in Figure 9. For values of [**1**] less than 0.7 mM, hydrogen production after 5 h of photolysis exhibits a distinctly linear dependence on [**1**]. However, further increases of the cobalt concentration above 0.7 mM led to an essentially constant rate of H_2 generation, consistent with the photochemical steps becoming turnover-limiting at these values of [Co]. Similar experiments have been reported recently by the groups of Alberto and Artero for a related system in which the chromophore employed was $ReBr(CO)_3(bpy)$.[34,36] The latter shows a linear dependence on Co concentration, while the former shows a quadratic dependence.

For the single-Co mechanisms, the rate constant should have a linear dependence on [Co], whereas for the two-Co mechanism, the rate should vary as $[Co]^2$. The results in Figure 9 clearly show a linear dependence of rate with [Co] at concentrations below 0.7 mM and thus support a

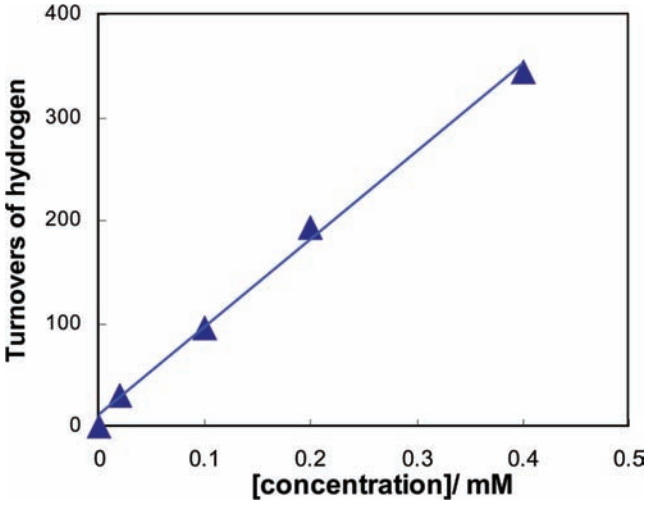

Figure 9. Hydrogen production under different concentrations of cobalt complex **1** (together with 1.1×10^{-5} M Pt chromophore **C1** and 1.6×10^{-2} M TEOA at pH = 8.5).

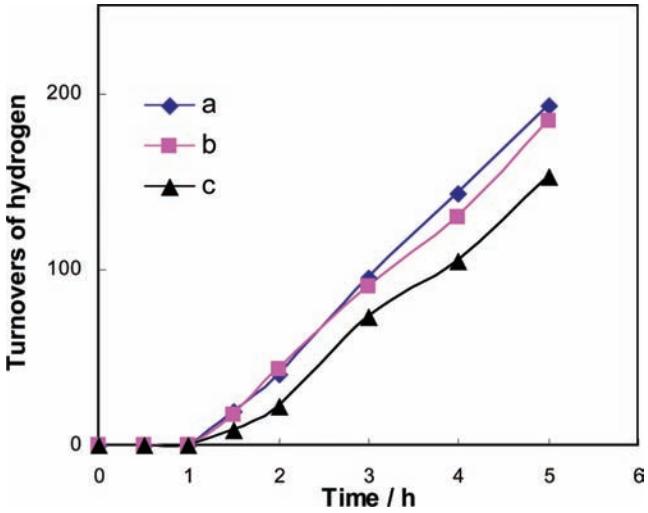

Figure 10. Mercury test for hydrogen production under the following conditions: 1.1×10^{-5} M Pt chromophore **C1**, 1.6×10^{-2} M TEOA, and 2.0×10^{-4} M complex **1** at pH = 8.5, (a) without mercury, (b) with 3 mL of mercury, and (c) pretreated with mercury (3 mL) overnight, then filtering off the mercury prior to photolysis.

single-Co mechanism for hydrogen formation in the present photochemical system. While the two single-Co mechanisms mentioned above are kinetically indistinguishable at this point, we favor the one involving Co (III) hydride reduction to Co(II) hydride followed by protonation because of favorable charge management in this mechanism that results from alternate e^- and H^+ additions.

Experimental observations in support of both single Co and two Co mechanisms for hydrogen generation have been presented in the literature. Artero et al. have suggested the single-Co mechanism in which the Co(III) hydride reacts with H^+ to form H_2 in the nonaqueous electrochemical system using $[Co(dmgBF_2)_2(OH_2)_2]$ as the catalyst with the weak acids p-cyanoanilinium and $[Et_3NH]^+$ as the proton source, while Peters et al.[30] favor the two-Co mechanism for the same catalyst with stronger acids such as HBF_4, TsOH, CF_3COOH, and AcOH based on electrochemical modeling. Alberto et al.[36] also favor the two-Co mechanism for their nonaqueous photochemical system in which strong acid is used as the proton source. In fact, both single-Co and two-Co mechanisms may be operating in all of these systems to differing respects, depending on conditions.

A distinction for the photochemical system reported here is that water is an integral part of the system and photochemical H_2 evolution is most active under weakly basic conditions, maximizing at pH 8.5. The protonation of Co(I) to form the Co(III) hydride at this pH requires that the Co(I) species be moderately basic. This requirement does not exist for the systems in which strong acid is used as the proton source. While most of the work using Co molecular catalysts for H_2 generation has emphasized the low overpotential for hydrogen evolution and the consequent low potential for the reduction of Co(II) to Co(I), in the present system, the basicity of the Co(I) species is important and may explain why the difluoroborylated complex **7** does not function as a catalyst in the photochemical system reported here.

We have previously written that purported molecular catalysts for hydrogen evolution actually served as colloidal precursors through photochemical decomposition, and that it is therefore important to rule out the existence or formation of colloids in any photochemical system for making hydrogen.[53] Consequently, experiments were run to determine if colloidal cobalt was possibly formed and acted as the real catalyst in the present photochemical system. For these experiments, elemental mercury was used. Mercury is known to poison or inhibit the activity of metal catalysts including colloids[54,55] and forms an amalgam with cobalt.[56] Two photolyses were done in addition to a parallel run of the system described here (1.1×10^{-5} M chromophore **C1**; 1.6×10^{-2} M TEOA; 2.0×10^{-4} M Co(III) complex **1** in MeCN/water (3:2 v/v) at pH = 8.5). In one, elemental mercury was added to the **C1** + **1** + TEOA reaction system (~3 mL with vigorous stirring) throughout the course of photolysis. In the second, the same system was stirred over Hg for 12 h, after which the mercury was removed and photolysis was started. The results are shown in Figure 10. The samples with and without Hg throughout the course of the photolysis gave nearly identical results, while the sample pretreated with mercury before photolysis yielded a slightly lower value, possibly because of minor losses of the starting solution during filtration. Overall, the results are consistent with the absence of any effect of the added mercury and thus support the notion that in this system the cobaloxime complexes are indeed the active catalysts.

Conclusion. The cobaloxime complexes **1**−**7** act as oxidative quenchers of photoexcited Pt chromophore **C1**. Quenching studies and Stern−Volmer analysis reveal that all of the complexes except for **5** exhibit near diffusion-controlled rates of quenching; for **5**, the quenching rate constant is slower at 4.0×10^7 M^{-1} s^{-1}. In a system composed of a Pt(II) terpyridyl acetylide or cyclometa-

(53) Du, P.; Schneider, J.; Li, F.; Zhao, W.; Patel, U.; Castellano, F. N.; Eisenberg, R. *J. Am. Chem. Soc.* **2008**, *130*, 5056–5058.
(54) Anton, D. R.; Crabtree, R. H. O. *Organometallics* **1983**, *2*, 855–859.
(55) Paul, F.; Patt, J.; Hartwig, J. F. *J. Am. Chem. Soc.* **1994**, *116*, 5969–5970.
(56) Paklepa, P.; Woroniecki, J.; Wrona, P. K. *J. Electroanal. Chem.* **2001**, *498*, 181–191.

lated phenyl−bipyridyl acetylide chromophore, TEOA, and complexes **1**−**5**, the photogeneration of H_2 is observed. All of the chromophores **C1**−**C7** work for photoinduced hydrogen production. While most of the studies of hydrogen photogeneration were done with chromophore **C1** and Co catalyst **1**, comparative runs show that chromophore **C4** and cobaloxime catalyst **2** are most effective. The rate of H_2 evolution is dependent on solution pH, TEOA concentration, and the ratio of $MeCN/H_2O$ with more than 2100 turnovers obtained in 10 h of irradiation ($\lambda > 410$ nm) using **C1** and **1** in $MeCN/H_2O$ (24:1 v/v).

Spectroscopic and mechanistic studies of the system reveal an induction period to hydrogen evolution and an initial color change to bright yellow characteristic of Co (III) reduction to Co(II). Hydrogen is usually produced after 1−2 h of photolysis with $\lambda > 410$ nm when [TEOA] $= 1.6 \times 10^{-2}$ M. Mechanistically, further reduction to Co (I) occurs, followed by protonation to form a Co(III) hydride intermediate. Variation of catalyst concentration reveals a linear relationship with H_2 evolution that is consistent with a mechanism involving only a single Co for H_2 generation. We propose that the mechanism proceeds by reduction of the Co(III) hydride intermediate and subsequent reaction with H^+ to give H_2 with regeneration of the Co(II) catalyst. Ironically, $[Co(dmgBF_2)_2(OH_2)_2]$ (**7**), which is most effective in the *electro*catalytic reduction of H^+ to H_2, does not work in the present system, in part due to the Co(II)/Co(I) reduction potential, which is too positive to achieve proton reduction at pH 7−8.5.

Acknowledgment. We wish to thank the Division of Basic Sciences, U.S. Department of Energy for financial support of this research (DE-FG02-90ER14125). P.D. gratefully acknowledges an Arnold Weissberger Fellowship.

Note Added after Print Publication. The print publication of June 1, 2009 (Vol. 48, issue 11), contained incorrect data in Scheme 1 and Table 4 on pp 4952–4962. These were corrected on the web version on August 31, 2009. An Addition and Correction also appears in the August 31, 2009 (Vol. 48, issue 17), print issue.

Supporting Information Available: X-ray crystallographic data of complexes **2** and **3** in CIF format. This material is available free of charge via the Internet at http://pubs.acs.org/.